The analysis of x-ray absorption fine structure: beam-line independent interpretation

J L Glover and C T Chantler

School of Physics, University of Melbourne, Victoria 3010, Australia

E-mail: chantler@ph.unimelb.edu.au

Abstract

Can current experimental techniques and analytical procedures produce x-ray absorption fine structure (XAFS) which is independent of the beam line or synchrotron used? We investigate the consequence upon XAFS interpretation of typical systematic errors, including determination of the edge energy, detector response and synchrotron bandwidth. Using the highest accuracy data set of the mass-attenuation coefficient collected so far, we consider a series of systematic effects in the analyses of both the near-edge and extended energy regions of the spectrum. We investigate whether conclusions derived from an experiment using a given analytical procedure are consistent when performed on different synchrotron beam lines. We find that the effectiveness of common XAFS analysis is limited by experimental and data reduction techniques, particularly relating to determinations of photon energy. By correcting for all major systematic errors in XAFS data, one can determine bond lengths more robustly and with greater accuracy.

Keywords: XAFS, atomic and solid state physics, systematic error, bandwidth, edge energy, detector response

1. Introduction

X-ray absorption fine structure (XAFS) analysis is one of the dominant techniques at synchrotrons for local order and structural identification, with hundreds of papers published each year [1, 2]. However, despite the maturity of the field and the empirical nature of the analytical techniques, the effect of experimental uncertainty and analysis errors are poorly understood and often neglected. Here we investigate the robustness of XAFS analytic techniques when well-defined systematic effects are introduced. In general, these systematic contributions are present in most data sets.

The data used for this investigation were measured using the x-ray extended-range technique (XERT) [3, 4] and is of the molybdenum K-edge [5] at a temperature of $27 \pm 1.5°$ C. The energy range of the data is 18 939–22 011 eV; the region just above the K-edge is illustrated in figure 1.

This XERT approach characterizes and corrects for systematic errors such as dark current, air attenuation, harmonics, bandwidth and scattering. The resulting experimental accuracy for the Mo data set is between 0.02% and 0.15% with most of the points having an accuracy of 0.02%. This makes it the most accurate mass-attenuation data published, and hence ideal for this investigation.

The data have an absolute energy calibration, which means the energy was determined directly from a germanium crystal mounted on a Huber four-circle diffractometer [5] and is accurate to between 0.0018% and 0.0025%. This has the advantage that the energy is not tied to the interpretation of any XAFS feature or the stability and purity of a reference foil.

In this paper, we consider the impact of several systematic errors upon typical analytical procedures and results for such a data set. Hence we gauge how these analytical techniques are affected by the systematics. These illustrations prove the magnitude of typical effects on derived results and thereby provide a caution to current interpretation and error analyses.

We consider (section 2) standard XAFS processing of experimental data, comparing such results to crystallographic
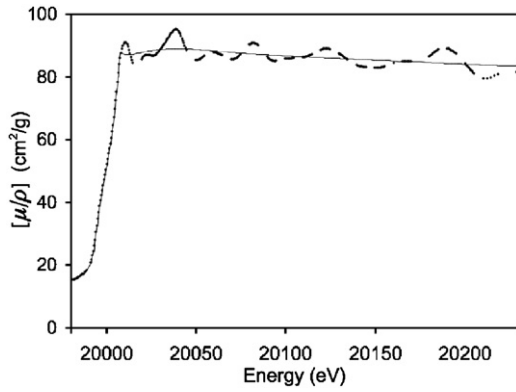
Figure 1. Mass-attenuation coefficient of molybdenum in the region of the K-edge. Error bars of 0.02% are smaller than the size of the dots. The thin line shows the XAFS background spline.

determinations of the molybdenum lattice parameter. We detail the process to analyse XAFS data and apply it to molybdenum. The effect of uncertainties in E_0 are particularly considered, which can lead to errors of up to 3–4% in derived radii. In section 3, the effect of certain aspects of detector response are considered. Section 4 looks at the effect of synchrotron bandwidth on XAFS analysis. Using the information detailed in previous sections, we conclude by discussing how to obtain high-quality beam-line independent results, which can resolve these issues for this major field and for applications to other fields.

2. XAFS analysis of molybdenum

A standard radial Fourier transform analysis was performed on the molybdenum data. The base line absorption was characterized by fitting a spline function ($\mu_0(E)$) to the data, such that the low-frequency components of the Fourier transform were minimized. We used a popular computer implementation of this method known as IFEFFIT [6], which uses the FEFF engine [7]. While other implementations exist, the choice of approach does not affect any conclusions of this paper.

Determination of the absorption edge energy is usually found by looking for a maximum, denoted by E_{inf}, in the derivative of $\mu(E)$. It is important to separate the idea of an experimentally-determined coefficient (denoted by E_0 in IFEFFIT) from the true theoretical absorption edge energy, which we will here denote as E_i. $\chi(k)$, the fine structure function, is then calculated as follows:

$$\chi(k) = \frac{\mu(E) - \mu_0(E)}{\Delta\mu(E_0)}, \tag{1}$$

$$k = \frac{2\pi}{h}\sqrt{2m_e(E - E_0)}, \tag{2}$$

where $\mu_0(E)$ is a smooth atom-like background, $\Delta\mu(E_0)$ is the edge height, k is the photoelectron wavenumber and E_0 is the energy of the edge.

There are a number of definitions of E_0 and it is not clear where the 'correct' assignment of E_0 is relative to the edge. For example, the first inflection point of a metallic foil K-edge may be close to the Fermi energy while the Fermi

energy for L3 edges of nearly d-band filled transition metals may be near the peak of the white line. We use the most common procedure, by first approximating E_0 with the edge inflection point energy, E_{inf}.

The Fourier transform of $\chi(k)$ is $\chi(R)$. Peak positions in $\chi(R)$ are generated by the surrounding atoms, from which bond lengths can be derived. This determination of local environmental radii is one of the primary purposes of XAFS analysis. Other related parameters including local geometry (cubic, trigonal, etc), next-nearest neighbours, ionization states and bonding can also be determined by XAFS analysis. By fitting the fine-structure function $\chi(k)$ to a defined theoretical prediction from FEFF 8.2, refinement codes such as IFEFFIT are able to derive bond lengths and other useful parameters.

The most precise determination of this radius using XAFS [8] yields a lattice parameter of $a_0 = 3.1530 \pm 0.0003$ Å corresponding to nearest neighbour distances of 2.731 ± 0.0003 Å, 3.153 ± 0.0003 Å and 4.459 ± 0.0005 Å. This analysis assumed a body-centred cubic geometry and propagated errors carefully. These uncertainties neglect possible scaling which would raise the uncertainty to 0.003 Å or 0.1%. E_0 was determined to be 19 996.88 eV, the Debye temperature was fitted to be 360 K and S_0^2 was found to be 1.153.

2.1. Comparison to crystallography

X-ray crystallography has determined that in crystalline samples the three nearest neighbour bond-lengths are 2.725 Å ($\sqrt{3}a_0/2$), 3.147 Å (a_0) and 4.451 Å ($\sqrt{2}a_0$) [9] following the bcc structure. Variation in a_0 between different reported values is 0.0004 Å and may be interpreted as a typical uncertainty. Simple crystallographic error estimates provide a statistical precision but may underestimate systematic uncertainty. However, the results of this analysis indicate agreement between XAFS and crystallographic determinations to 0.006 Å or 0.2%. This is consistent with the different nature of the two probes which measure different quantities [10, 11]. Bond-length determinations of this accuracy can only arise from data free from the major effects of systematic error.

Of course, Bragg diffraction formally measures the distance between average positions, $R_c = |\langle r_2 - r_1 \rangle|$ (or 'apparent' bond-length), whereas XAFS measures the average interatomic distance, $\langle r \rangle = \langle |r_2 - r_1| \rangle$. Therefore, bond lengths measured by XAFS should exceed those measured by x-ray diffraction by $\langle r \rangle - R_c = \frac{\langle \Delta u_\perp^2 \rangle}{2R_c} + \cdots$.

2.2. Determination of bond lengths

The first inflection point energy, E_{inf}, was found to be 20 006 eV, corresponding to the location of the prominent maximum in the derivative of $\left[\frac{\mu}{\rho}\right](E)$. The fit was carried out for the 16 shortest unique paths (i.e. the local geometry was not assumed to be bcc), with a single many-body amplitude reduction factor (S_0^2) for all paths. Thermal effects were treated using Debye–Waller factors, modelled using the correlated Debye model leaving the Debye temperature θ_D as a fitting parameter.

Avoiding the assumption of a bcc lattice leads to independently fitted nearest neighbour distances. E_0 was then refined to $20\,006.9 \pm 0.5$ eV, and the first three independent nearest neighbour distances were fitted to be 2.767 ± 0.007 Å, 3.217 ± 0.012 Å and 4.361 ± 0.164 Å. These quoted uncertainties are the output of the fitting program but should *not be considered* to correspond to a standard deviation (because the input experimental uncertainties are not propagated by the code) [8]. When the correct (bcc) geometry is not assumed, the uncertainty in resultant parameters increases dramatically.

The experimental data have an accurate absolute calibration of energy, so that one need not fit for the ionization energy (E_i), if theory can provide a correspondingly accurate value. The highest precision calibrated reference value for the Mo K inflection point E_{inf} is $20\,000.36 \pm 0.02$ eV [12]. This precision is excellent but E_{inf} can be affected by bandwidth and is not necessarily a robust definition of the absorption edge itself. Our data suggest $E_{\text{inf}} = 20\,006$ eV with a small error bar, while the original reference [13] provides the earlier calibrated value as $20\,004.3 \pm 0.3$ eV, which is clearly discrepant and implies beam-line or sample dependence. For this reason alone, independent absolute energy calibration is important.

By constraining E_0 to $20\,000.36 \pm 0.02$ eV, we improve the precision of the nearest neighbour distances considerably to 2.748 ± 0.001 Å, 3.142 ± 0.003 Å and 3.780 ± 0.025 Å. Having an absolute energy calibration and so being able to constrain E_0 reduced the relative uncertainty of the inner shell radius by a factor of 7. Furthermore, in this case a more accurate bond length was possible with an *a priori* understanding of the local symmetry.

2.3. Correlation of bond lengths to E_0

When a relative energy calibration is used, the edge energy must become an experimental parameter to be determined. However, we have shown that it is possible to obtain values for E_0 varying by 10 eV in different refinements, even for the *same high-quality data set*. Separate from this issue is the experimental energy hysteresis, where the energy readout from the synchrotron monochromator can shift between scans, particularly after a beam dump. As a result of these effects, errors in the energy of the edge do occur. A recent study [14] has observed that out of 14 manuscripts surveyed, only 4 had ΔE_0 shifts less than 10 eV, 3 had discrepancies larger than 10 eV and 7 manuscripts provided no values for E_0 or ΔE_0. Consequently, we now investigate what effect such an error in E_0 might have on parameters derived from an XAFS analysis.

In all XAFS analysis, a systematic offset in E_0 is linearly proportional to the corresponding change in the determined radii from the radial density distribution in $\chi(R)$. We illustrate the situation for a shift of 10 eV, but the structural effects can be scaled by the reader if a shift of 5 eV or 15 eV were assumed instead.

We explicitly changed E_0 by differing amounts ΔE_0. As a result the locations of peaks in $\chi(k)$ are affected significantly (figure 2). It also leads to a dramatic alteration of $\chi(R)$ (figure 3). We note the expected strong negative correlation between E_0 and the nearest neighbour distance.

When E_0 was altered by only 10 eV (0.05%), it resulted in a 3.5% change in the location of the peak corresponding to the
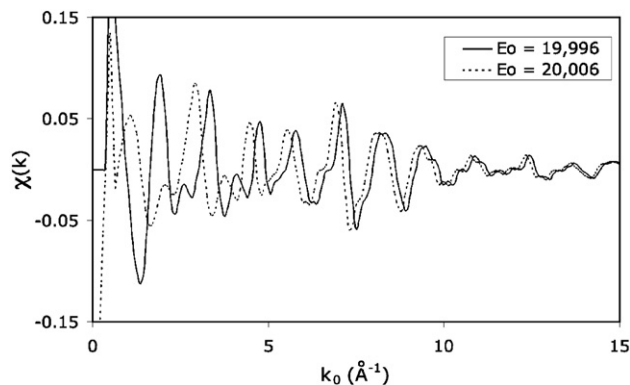
Figure 2. $\chi(k)$ calculated using $E_0 = 20\,006$ eV and $E_0 = 19\,996$ eV. The low-k region of $\chi(k)$ is greatly affected.
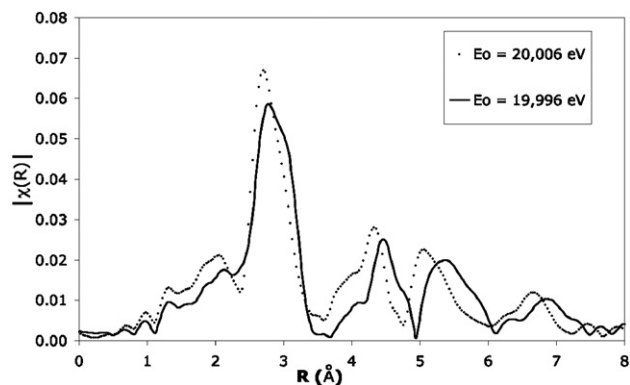

Figure 3. $|\chi|$ as a function of R, calculated using $E_0 = 20\,006$ eV and $|\chi(R)|$ calculated using $E_0 = 19\,996$ eV. The effect on the low-k region of $|\chi(R)|$ shifts the resulting radial distances linearly with the energy offset error.

nearest neighbour atom. Small errors in the determination of the edge energy can therefore result in large errors in derived parameters. A recent work in *Nature* [15] has noted that their potential conclusions regarding relative interatomic distance determination are compromised by an error or energy shift of as little as 0.01 eV. Problems resulting from an incorrect determination of the edge energy need not occur in data with an accurate absolute energy determination.

3. Detector response

There are effects in some XAFS data caused by detector response rather than the interaction between x-rays and the sample, which need to be quantified and compensated for. An argon-gas ion-chamber measures x-ray beam intensity. However, when such a device is isolated from all x-ray sources it still gives a non-zero reading due to electronic noise and amplification. This *dark current* is a common feature of all detectors. While some beam lines make offset measurements, many do not asses the accuracy of such tests and numerous beam lines do not collect these data at all. It is therefore important to understand what effect dark current has on XAFS analysis.

In the case of strongly attenuating samples, correcting for the dark current of the downstream detector becomes
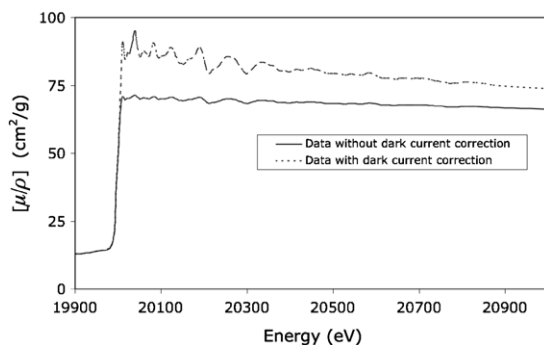
Figure 4. The molybdenum experimental data are plotted with a simulation of the effects of neglecting the dark current analysis for 100 μm samples. Neglecting the dark current analysis has greatly damped the fine structure. While this particular thickness is relatively large, the qualitative effect remains for all thicknesses.

Figure 5. $|\chi(R)|$ is plotted with and without bandwidth effects. The non-uniform relative heights of the peaks illustrates how bandwidth weakens high-frequency XAFS information and hence damps the higher R structure.

extremely important. The molybdenum data used in this section have been corrected for dark current effects, so we use a simple model to simulate the effects of failing to correct for this. A typical upstream count rate for the experiment of 500 000 counts per second and a typical dark current of 300 ± 10 counts per second in both detectors were assumed [5].

The sample in figure 4 was assumed to be 100 μm thick (i.e. highly absorbing, $\log_{10}\left(\frac{I_0}{I}\right) \approx 4$), to emphasize the potential effect of neglecting dark current. This thickness corresponds to the thickest sample used in the XAFS region from the experiment which produce these data. Although it is possible to choose thicknesses where this effect is not so extreme, it is impossible to have a single optimum thickness above and below the edge.

Without correction for the dark current, the edge height is dramatically decreased (see figure 4) and the magnitude of the XAFS oscillations has been greatly damped. This clearly destroys much information derivable from a radial Fourier transform analysis.

Poor treatment of dark current can all but destroy the usefulness of $\chi(k)$, for quantitative or even qualitative comparison in some situations. In our investigation, even 50 μm and 75 μm thicknesses reveal very large and compromising effects on the $\chi(k)$ structure by failing to correct for dark current. This effect cannot be compensated for with background subtraction procedures.

4. Bandwidth

There are numerous spectrum-broadening mechanisms including hole widths and inelastic mean free paths [16] but these processes are intrinsic to the sample and should be modelled by theory. However, a synchrotron is a wideband source, and a range of common x-ray monochromation methods results in a beam with a bandwidth of a few eV [17]. The effect of x-ray bandwidth on an XAFS analysis is considered here. The molybdenum data have been corrected for bandwidth effects using a linearized deconvolution [18]. The energy beam profile after monochromation was found to be a Gaussian of width 1.6 eV [18]. In some situations the bandwidth can be much higher than this [19], and is normally energy-dependent. In a recent
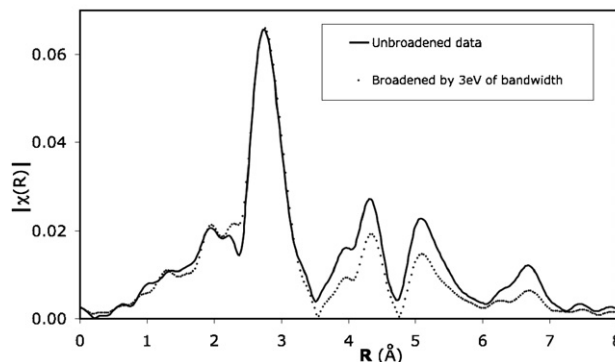
powder diffraction work [20], the measured bandwidth varied from 2 eV at an energy of 6 keV, up to 6 eV at an energy of 20 keV.

The effect of bandwidth was simulated by convolving the current data with a 3 eV Lorentzian. Although slightly larger than the bandwidth seen during this particular molybdenum experiment, such a bandwidth is common at numerous beam lines (and the observed effects scale). An XAFS analysis on the data yielded found including bandwidth broadening resulted in a change in peak locations of less than 1%. Hence modest bandwidth might not affect the location of transformed peaks in R space.

However, bandwidth distorts the high-frequency information in XAFS. To see this we look at $|\chi(R)|$, the Fourier transform of $|\chi(k)|$, shown in figure 5. The convolved spectrum has been normalized so that the height of the largest peak is the same as the unconvolved spectrum. The higher frequency ($R > 3.5$ Å) peaks are greatly damped, with the peak at 6.7 Å having lost half its amplitude. Hence, interpretation using standard XAFS analytical codes is compromised and easily leads to errors in coordination number, phase offsets or amplitude coefficients for the longer paths.

There will generally be some modest bandwidth in synchrotron experiments. Characterization of the bandwidth allows one to correct for and draw more reliable conclusions from a XANES analysis. Bandwidth can also distort the absorption edge, making the edge energy E_0 more difficult to determine. This again highlights the advantage of an absolute energy calibration.

5. Conclusion and outlook

Systematic errors such as poor determination of the edge energy, inaccurate energy calibration, bandwidth and the effects of dark current can affect XAFS analysis strongly. Despite this, many XAFS papers do not measure or correct for these systematic errors, and many experimental geometries are unable to estimate them. These systematic effects vary between beam lines. Hence, a result from one beam line may not be portable to another, and this limits the value of a particular publication for the wider community.

The systematic errors investigated in this paper can be characterized and compensated for if good experimental procedures and data analysis techniques are used. To minimize these effects, an experiment determining $\left[\frac{\mu}{\rho}\right]$ needs an accurate, well-calibrated and absolute energy determination. Effects of energy offset, bandwidth and dark current should be quantified and corrected for.

The x-ray extended range technique (XERT) [3, 5, 21] satisfies these criteria and has provided highly accurate measurements of $\left[\frac{\mu}{\rho}\right]$. The XERT uses multiple samples (a minimum of three) covering a broad range of log-attenuation ratios, so that dark current, harmonic contamination, bandpass and other nonlinearities may be characterized by orthogonal signatures and hence directly measured in the experiment. XERT has been used in fluorescence mode and for dilute systems, and can be easily modified for use in a wide range of experimental setups. The technique covers a very wide range of energy (typically 10 keV) so that energy-dependent systematics can be recognized and controlled. The method requires an independent calibration of energy separate from the nominal or calibrated monochromator encoder reading, and separate from any use of white line markers as transfer standards.

One of the great opportunities of XAFS is to determine local ordering, bond distances, geometry, oxidation state and general bonding patterns. However, uncertainties and hence interpretational problems arise from the effects discussed here which can be more significant than has been generally appreciated. While analysis and theory are developing strongly, this paper highlights the need for carefully measured and calibrated experimental data.

Acknowledgments

References

[1] Hasnain S S, Helliwell J R and Kamitsubo H 1999 *J. Synchrotron Radiat.* **6** 121–2
[2] Hedman B and Pianetta P 2006 *AIP Conf. Proc.* **882** xxi–xxii
[3] Chantler C T, Tran C Q, Barnea Z, Paterson D, Cookson D J and Baliac D X 2001 *Phys. Rev.* A **64** 062506
[4] Tran C Q, Chantler C T and Barnea Z 2003 *Phys. Rev. Lett.* **90** 257401
[5] de Jonge M D, Tran C Q, Chantler C T, Barnea Z, Dhal B B, Cookson D J, Lee W K and Mashayekhi A 2005 *Phys. Rev.* A **71** 032702
[6] Newville M 2001 *J. Synchrotron Radiat.* **8** 322
[7] Ankudinov A L, Ravel B, Rehr J J and Conradson S D 1998 *Phys. Rev.* B **58** 7565
[8] Smale L F, Chantler C T, de Jonge M D, Barnea Z and Tran C Q 2006 *Radiat. Phys. Chem.* **75** 1559–63
[9] Taylor A, Doyle N J and Kagle B J 1961 *J. Less-Common Met.* **3** 265
[10] Fornasini P, a Beccara S, Dalba G, Grisenti R, Sanson A, Vaccari M and Rocca F 2004 *Phys. Rev.* B **70** 174301
[11] Vaccari M, Grisenti R, Fornasini P, Rocca F and Sanson A 2007 *Phys. Rev.* B **75** 184307
[12] Deslattes R D, Kessler E G, Indelicato P, de Billy L, Lindroth E and Anton J 2003 *Rev. Mod. Phys.* **75** 35
[13] Kraft S, Stumpel J, Becker P and Kuetgens U 1996 *Rev. Sci. Instrum.* **67** 681
[14] Ravel B and Kelly S D 2006 *AIP Conf. Proc.* **882** 132–4
[15] Pettifer R F, Mathon O, Pascarelli S, Cooke M D and Gibbs M R J 2005 *Nature* **435** 78
[16] Bourke J D, Chantler C T and Witte C J 2007 *Phys. Lett.* A **360** 702–6
[17] de Jonge M D, Barnea Z, Tran C Q and Chantler C T 2004 *Phys. Rev.* A **69** 022717
[18] de Jonge M D 2005 *Doctoral Thesis* University of Melbourne
[19] van Dorssen G E, Koningsberger D C and Ramaker D E 2002 *J. Phys.: Condens. Matter* **14** 13529–41
[20] Rae N A, Chantler C T, Tran C Q and Barnea Z 2006 *Radiat. Phys. Chem.* **75** 2063
[21] Tran C Q, Chantler C T, Barnea Z, de Jonge M D, Dhal B B, Chung C T Y, Paterson D and Wang J 2005 *J. Phys. B: At. Mol. Opt. Phys.* B **38** 89–107